

MorFiC: Fixing Value Miscalibration for Zero-Shot Quadruped Transfer

Prakhar Mishra^{1,*}, Amir Hossain Raj², Xuesu Xiao², and Dinesh Manocha¹

¹University of Maryland, College Park, MD, USA

²George Mason University, Fairfax, VA, USA

*Collaborating Researcher; M.Eng. University of Maryland, 2023

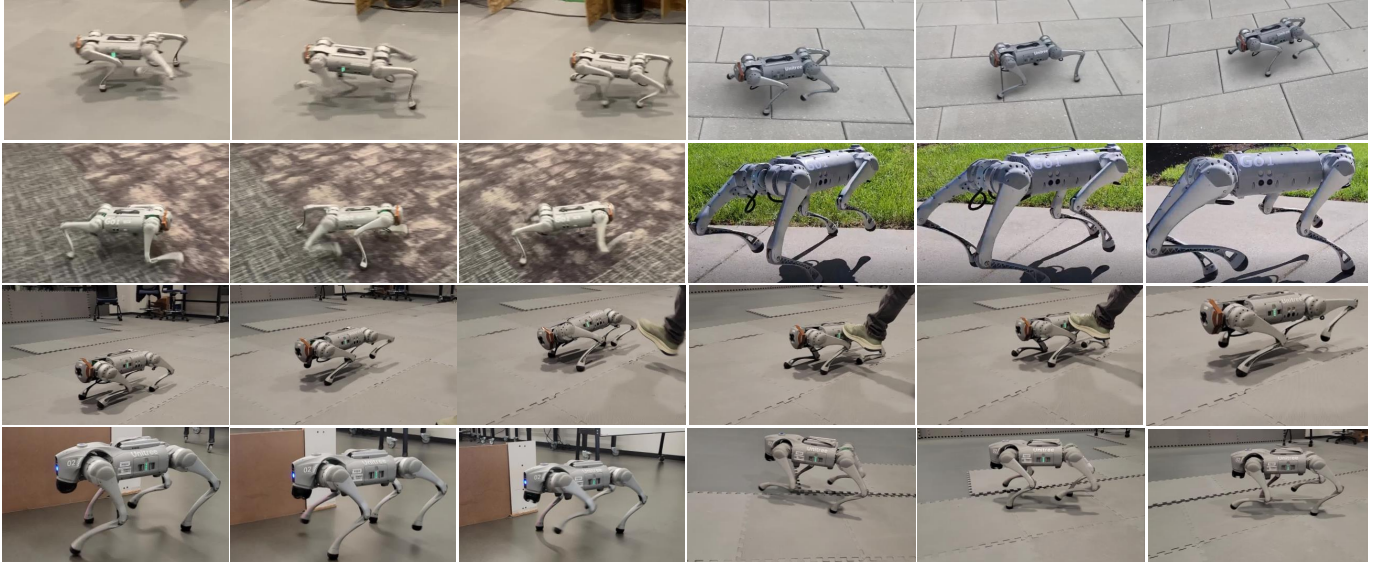


Fig. 1. We present **MorFiC**, a reinforcement learning framework for cross-morphology locomotion that trains a single policy on one source quadruped and transfers it to other robots with different morphologies (e.g., different mass distributions, joint limits, and actuation constraints) without retraining, by improving how the *value function* generalizes under morphology shift using a morphology-aware FiLM-modulated critic. Real-world deployment on a Unitree Go1: MorFiC runs stably at ≈ 1.4 – 1.7 m/s without task-specific fine-tuning. *Top two rows*: representative Go1 roll-outs (indoor and outdoor). *Third row*: push-disturbance recovery on Go1. *Bottom row*: Zero-shot deployment on Unitree Go2 (runs at ≈ 1.1 – 1.3 m/s) using the same trained policy weights.

Abstract—Generalizing learned locomotion policies across quadrupedal robots with different morphologies remain a challenge. Policies trained on a single robot often break when deployed on embodiments with different mass distributions, kinematics, joint limits, or actuation constraints, forcing per-robot retraining. We present MorFiC, a reinforcement learning approach for zero-shot cross-morphology locomotion using a single shared policy. MorFiC resolves a key failure mode in multi-morphology actor-critic training: a shared critic tends to average incompatible value targets across embodiments, yielding miscalibrated advantages. To address this, MorFiC conditions the critic via morphology-aware modulation driven by robot physical and control parameters, generating morphology-specific value estimates within a shared network. Trained with a single source robot with morphology randomization in simulation, MorFiC can transfer to unseen robots and surpasses morphology-conditioned PPO baselines by improving stable average speed and longest stable run on multiple targets, including speed gains of +16.1% on A1, $\approx 2\times$ on Cheetah, and $\approx 5\times$ on B1. We additionally show that MorFiC reduces the value-prediction error variance across morphologies and stabilizes the advantage estimates, demonstrating that the improved value-function calibration corresponds to a stronger transfer performance. Finally, we demonstrate zero-shot deployment on two Unitree Go1 and Go2 robots without fine-tuning, indicating that critic-side conditioning is a practical

approach for cross-morphology generalization.

I. INTRODUCTION

Reinforcement learning has allowed quadrupedal robots to achieve agile and robust locomotion across a wide range of speeds, terrains, and disturbances. Using large-scale simulation and massively parallel training, recent methods have demonstrated behaviors that are difficult to obtain through classical model-based control alone [1, 2, 3]. Despite this progress, most of the learned locomotion policies remain tightly coupled to a single robot embodiment. Even within the same family of quadrupeds, policies trained on one platform often fail when deployed on another [4], substantially limiting policy reuse and increasing the deployment cost.

Generalizing locomotion policies across robot morphologies is challenging because relatively small changes in physical structure, such as mass distribution, joint limits, or actuation capacity, can significantly alter the underlying dynamics [5]. Policies trained on a single robot tend to exploit morphology-specific regularities, which leads to brittle behavior when transferred to robots with different physical properties. AI-

though domain randomization improves robustness to modeling errors and facilitates sim-to-real transfer [6, 7, 8], it does not explicitly address systematic shifts in dynamics caused by morphology variation. As a result, policies often degrade sharply when evaluated in robots whose morphology lies near or beyond the boundary of the training distribution.

A natural response to this limitation is to condition policies on explicit morphology descriptors, *i.e.*, a vector of robot physical and control parameters (e.g., masses, joint limits, torque limits). Previous work has shown that providing physical parameters or learned embodiment representations can enable a single policy to control multiple quadrupedal robots [9, 10, 11]. These approaches demonstrate that morphology-aware policies can generalize within a limited range of embodiments. However, in practice, reliable zero-shot transfer remains difficult, particularly for robots that differ substantially from those seen during training. In many cases, morphology-conditioned policies achieve conservative behavior or reduced performance in unseen robots, suggesting that conditioning alone is insufficient [12, 13].

We argue that this limitation arises not primarily from insufficient policy expressiveness but from miscalibrated value estimation (*i.e.*, the model’s predicted long-term return for a given state, action and morphology) across morphologies. We argue that policy is not the only component which should generalize, value function must generalize first. In standard actor-critic methods such as PPO [14], a single critic is trained to approximate expected returns in all training environments. When multiple morphologies are present, the same state can correspond to fundamentally different future outcomes depending on the robot’s physical properties. For example, a state that is recoverable for a lightweight robot may correspond to imminent failure for a heavier one. A shared critic is therefore forced to average incompatible value targets, inducing morphology-dependent bias in the value function. This bias propagates directly to the advantage estimates used for policy updates, destabilizing learning and disproportionately harming performance on edge-case morphologies [15].

Main Results and Contributions: In this work, we introduce **MorFiC**, a *Morphology-Aware FiLM Critic* for zero-shot generalizable quadruped locomotion. Our key novelty in MorFiC lies in the way that morphology information is incorporated into the critic. Rather than concatenating the morphology parameters with the input of the critic, MorFiC conditions intermediate features of the critic using feature-wise linear modulation (FiLM) driven by latent learned morphology [16]. This architectural choice allows the critic to represent distinct morphology-specific value landscapes within a single shared network while avoiding destructive interference between morphologies. By explicitly decoupling value estimation across robots, MorFiC directly corrects morphology-induced value bias and improves advantage calibration during training.

MorFiC is trained using explicit morphology randomization over physically significant ranges, for example masses, inertia, and joint torque limits, applied to a single robot template in simulation. Crucially, the resulting improvements do not

arise merely from exposure to more morphologies, but from more accurate and stable value estimation across them. This enables the policy to exploit the physical capabilities of each robot more effectively, resulting in higher achievable speeds on capable platforms and improved robustness on challenging or edge-case morphologies.

We evaluate MorFiC on a diverse suite of quadrupedal robots, including Unitree Go1, Go2, A1, B1, and the MIT Mini Cheetah, and compare against standard PPO baselines, morphology-conditioned critics, and representative multi-robot locomotion methods. Across all platforms, MorFiC consistently achieves higher maximum forward speeds, higher task success rates, and stronger zero-shot transfer performance, particularly on robots that differ significantly from the training morphology. We further demonstrate successful zero-shot deployment on a real Unitree Go1 robot without fine-tuning. Together, these results show that morphology-aware value learning, rather than increased policy complexity or online adaptation, is a critical and previously underexplored component for reliable cross-morphology locomotion.

Our contributions are summarized as follows:

- We identify morphology-dependent value bias as a key failure mode limiting zero-shot cross-morphology locomotion.
- We propose MorFiC, a FiLM-modulated critic architecture that enables morphology-specific value estimation within a single shared network.
- We show that correcting value-function bias leads to higher maximum speed, improved stability, and better generalization compared to prior morphology-conditioned and multi-robot methods (Fig. 4 & Table IV).
- We demonstrate strong zero-shot transfer across multiple quadrupedal robots in simulation and successful deployment on real hardware using a single policy trained on one robot template. MorFiC achieves $\approx 1.4\text{--}1.7\text{ m/s}$ on Unitree Go1 and $\approx 1.1\text{--}1.3\text{ m/s}$ on Go2 robot.

II. RELATED WORK

A. Learning-Based Quadrupedal Locomotion

Reinforcement learning has enabled quadrupedal robots to achieve agile and robust locomotion, including high-speed running and disturbance recovery, both in simulation and on hardware [3, 2, 17]. These successes are largely driven by large-scale simulation and careful reward design, but typically assume a fixed robot embodiment during training. As a result, the learned policies are highly robot-specific and often fail when deployed on robots with different morphologies. In contrast, MorFiC explicitly targets cross-morphology generalization by addressing value-function errors that arise when training across varying robot dynamics.

B. Morphology-Conditioned and Multi-Robot Policies

Several recent works explore generalizing locomotion policies across robot morphologies by conditioning on physical parameters or learned embodiment representations. GenLoco [9],

TABLE I
MORPHOLOGY RANDOMIZATION RANGES USED DURING TRAINING. ALL
PARAMETERS ARE SAMPLED INDEPENDENTLY FROM UNIFORM
DISTRIBUTIONS.

Segment	Mass	Joint limits	
	[kg]	min [rad]	max [rad]
Hip	[0.51, 0.70]	[-1.10, -0.80]	[+0.80, +1.10]
Thigh	[0.63, 1.15]	[-1.65, -1.05]	[+3.49, +4.05]
Calf	[0.06, 0.17]	[-2.72, -2.60]	[-0.95, -0.78]
Foot	[0.00, 0.06]	-	-
Base	[3.30, 6.92]	-	-

Body Transformer [10], and ManyQuadrupeds [11] demonstrate that a single policy can control multiple quadrupedal robots when provided with morphology information. However, these approaches rely on shared critics and assume that value functions generalize across morphologies through conditioning alone. MorFiC departs from this assumption by explicitly conditioning the critic architecture itself, enabling morphology-specific value estimation and reducing interference between morphologies. This leads to improved zero-shot performance, particularly OOD robots.

C. Adaptation-Based Generalization

Another line of work addresses embodiment and dynamics variation through online adaptation or system identification. Rapid Motor Adaptation (RMA) and related methods infer latent dynamics from observation history and adapt the policy during deployment [18, 19]. Although effective, these approaches introduce additional complexity of inference and rely on temporal adaptation. MorFiC instead improves generalization at training time by correcting value estimation across morphologies, achieving strong zero-shot transfer without online adaptation or recurrent policies.

D. Value Learning and Training Stability

Value-function accuracy is critical for stable actor-critic learning, yet its role in cross-morphology generalization has received limited attention in locomotion research. Previous work has shown that value misestimation can destabilize deep reinforcement learning [15], and recent studies highlight interference issues in shared critics in multiple tasks or environments [20]. MorFiC addresses this issue directly by identifying morphology-induced value bias and mitigating it through morphology-aware critic modulation, leading to more stable advantage estimates and improved policy optimization.

E. Sim-to-Real Transfer Across Morphologies

Sim-to-real transfer for legged locomotion is commonly based on domain randomization and robust policy learning [6, 7]. Recent work emphasizes the rapid deployment of RL policies on hardware [17]. MorFiC complements these approaches by showing that morphology-aware value learning improves not only sim-to-sim transfer across robots, but also zero-shot deployment on real hardware without fine-tuning.

III. PRELIMINARIES

This section fixes notation and formalizes multi-morphology locomotion as a parameterized control problem. It then isolates how value estimation errors arise under morphology variation in advantage-based actor-critic training, motivating MorFiC in Section IV.

A. Zero-Shot Cross-Morphology Evaluation

We consider quadrupedal locomotion under morphology variation. Each robot embodiment is identified by a vector of morphology parameters $m \in \mathcal{M}$ encoding physical and control properties (for example, mass distribution, joint limits, actuator limits). Training is performed on a morphology distribution $p_{\text{train}}(m)$, while evaluation is performed on a holdout morphology m^* without additional training, fine-tuning, or online adaptation. We refer to this protocol as *zero-shot cross-morphology* evaluation [9, 18].

B. Parameterized MDP for Multi-Morphology Locomotion

Locomotion across embodiments is modeled as a parameterized Markov Decision Process:

$$\mathcal{M}(m) = \langle \mathcal{S}, \mathcal{A}, P_m, r_m, \gamma \rangle, \quad (1)$$

where \mathcal{S} and \mathcal{A} denote the state and action spaces, P_m is the morphology-dependent transition kernel, r_m is the reward function and $\gamma \in (0, 1)$ is the discount factor. This formulation is closely related to contextual and hidden-parameter MDPs that model families of environments with shared structure but varying dynamics [21]. A common approach is to optimize a morphology-conditioned policy $\pi_\theta(a | s, m)$ by sampling $m \sim p_{\text{train}}(m)$ during simulation [22, 9].

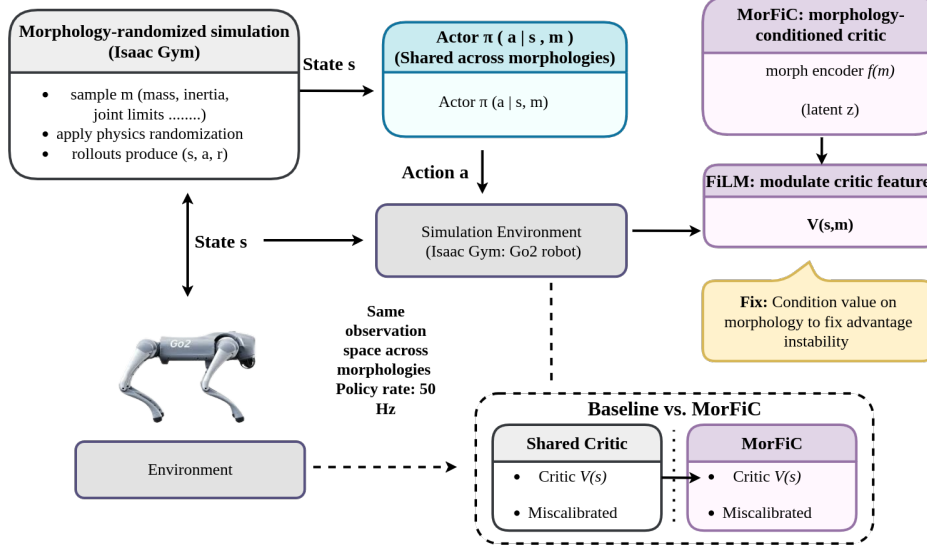
IV. MORFiC APPROACH

MorFiC is a morphology-aware actor-critic framework for zero-shot cross-morphology locomotion. The starting point is the failure mode in Section III: under morphology randomization, a shared critic tends to average incompatible value targets, which distorts advantages and destabilizes policy improvement. MorFiC addresses this by (i) explicitly sampling morphology and control parameters during training, and (ii) conditioning the critic through feature-wise linear modulation (FiLM) driven by a latent learned morphology [16]. The resulting critic represents $V(x, m)$ more faithfully, improving advantage calibration and allowing stronger zero-shot transfer.

A. Value Interference Under Morphology Variation

Multi-morph training aggregates roll-outs collected under a range of morphologies $m \sim p_{\text{train}}(m)$ and commonly fits a single critic using shared parameters. When identical inputs x_t correspond to different future outcomes under different morphologies, the value regression target becomes heterogeneous across m . A shared critic then tends to represent an average over incompatible value targets, yielding morphology-dependent value bias.

(i) Phase I: Train with morphology randomized dynamics and condition via FiLM to fix critic



(ii) Phase II Deployment

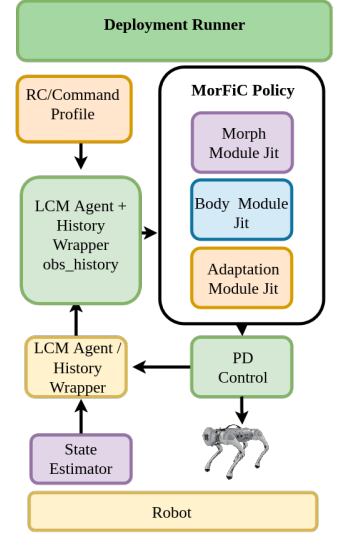


Fig. 2. Overview of MorFiC. First we sample morphology descriptor $m \sim p(m)$ and then apply it to the simulator (masses/inertia, joint limits/angles, torque limits, and PD/action scaling) to instantiate morphology-specific dynamics and generate roll-outs. After that we train a policy with PPO using a morphology latent $z = f(m)$; the critic is FiLM modulated by z to predict a morphology conditioned value and improve advantage estimates. Deployment (right) runs the trained JIT modules (morph encoder and body network, with optional adaptation) with an LCM based state estimator and RC/command profile input.

Such interference effects are well-known in multi-task and multi-domain learning with shared networks [23], and have been observed empirically in multi-robot locomotion policies [11]. In actor-critic methods, this mismatch is particularly consequential because the critic defines the baseline used in (3). Small morphology-dependent value errors can flip the sign or scale of \hat{A}_t , producing inconsistent updates across morphologies and brittle zero-shot behavior near the boundary of $p_{\text{train}}(m)$ (Fig. 3). This motivates conditioning the value pathway itself so that the critic can represent the morphology-specific return structure while retaining the efficiency of a single shared network.

B. Morphology Randomization and Episode Instantiation

At episode reset, each parallel environment samples a morphology $m \sim p_{\text{train}}(m)$ and applies it to the simulator, thus defining the morphology-dependent dynamics P_m in (1). The sampled m is kept fixed throughout the episode so that each rollout corresponds to a coherent robot instance. This episode-consistent randomization follows standard practice for robustness and transfer [8, 7, 6].

In this work, we use a simulator-supported morphology vector $m \in \mathbb{R}^{d_m}$ with parameters $d_m = 11$ (for example, link and base masses, joint-limit ranges). Each component is independently normalized to $[-1, 1]$ before being provided to the networks.

C. Morphology Latent Encoder

Rather than concatenating raw morphology parameters, MorFiC maps m to a learned latent representation

$$z = f_\psi(m), \quad z \in \mathbb{R}^{d_z},$$

using a lightweight MLP. The latent reduces scale mismatch across morphology dimensions and emphasizes morphology factors relevant for value learning. The same z is provided to both the actor and the critic.

D. FiLM-Modulated Critic

MorFiC conditions the critic by modulating intermediate critic features using FiLM [16]. Let the critic backbone compute features from the critic input stream $x_t := (o_t, h_t, p_t)$:

$$h = g_\phi(x_t).$$

A FiLM network maps z to affine feature-wise parameters

$$\gamma(z), \beta(z) = \text{FiLM}_\eta(z),$$

which produce modulated features;

$$\tilde{h} = \gamma(z) \odot h + \beta(z).$$

The value function is then predicted as

$$V_\phi(x_t, m) = v_\phi(\tilde{h}). \quad (2)$$

Compared to input concatenation, intermediate modulation allows the critic to represent a conditional family of value functions through morphology-dependent reparameterization of features, mitigating value interference across morphologies while retaining a single shared network.

E. Advantage-Based Actor-Critic Optimization

Policies are trained using advantage-based actor-critic methods, most commonly PPO [14]. Let \hat{G}_t denote an empirical return estimate. PPO updates the policy using advantage estimates

$$\hat{A}_t = \hat{G}_t - V_\phi(x_t), \quad (3)$$

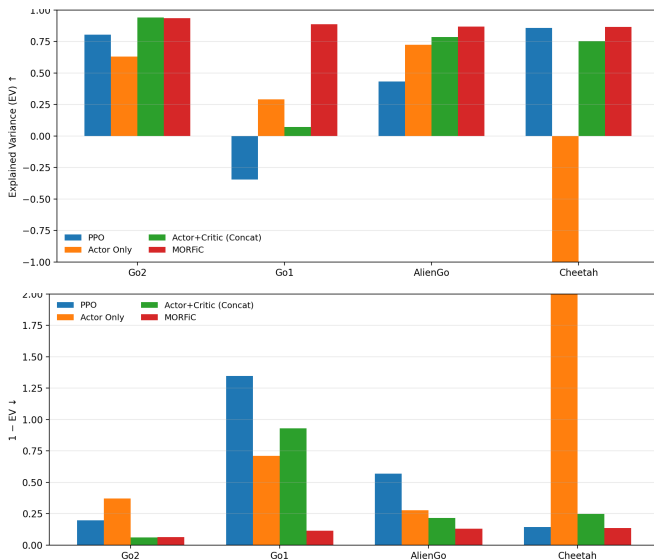


Fig. 3. Critic calibration and advantage stability under morphology shift. (a) Explained variance (EV) between bootstrapped returns and critic predictions across target robots; MorFiC maintains higher EV on out-of-distribution morphologies than PPO and morphology-to-policy baselines. (b) Advantage-noise proxy computed from the same rollouts; MorFiC reduces advantage noise on OOD robots, supporting the thesis that morphology-conditioned value calibration yields more stable updates and stronger zero-shot transfer.

where V_ϕ is a function of the learned value. In practice, generalized advantage estimation is widely used to compute \hat{A}_t with a favorable bias–variance tradeoff [24]. Because the advantage weights the policy gradient, the systematic value error directly alters the direction and magnitude of policy updates [14].

F. Policy and PPO Training Objective

The actor is conditioned on the same morphology latent and outputs actions as

$$a_t \sim \pi_\theta(a | o_t, z).$$

MorFiC is trained using standard PPO [14].

$$r_t(\theta) = \frac{\pi_\theta(a_t | o_t, z)}{\pi_{\theta_{\text{old}}}(a_t | o_t, z)}.$$

The clipped surrogate objective is

$$\mathcal{L}^{\text{clip}}(\theta) = \mathbb{E}_t \left[\min \left(r_t(\theta) \hat{A}_t, \text{clip}(r_t(\theta), 1 - \epsilon, 1 + \epsilon) \hat{A}_t \right) \right], \quad (4)$$

where advantages are computed using the morphology-aware critic:

$$\hat{A}_t = \hat{G}_t - V_\phi(x_t, m). \quad (5)$$

The value function is trained by regression to returns (with optional value clipping as in PPO) [14]. In addition to conditioning, MorFiC does not alter PPO; the change is the critic parameterization in eqn. 2, which improves the advantage calibration across morphologies.

TABLE II
OBSERVATION STREAMS USED FOR POLICY AND VALUE LEARNING.

Stream	Signals	Dim
o_t	$[v, \omega, g_{\text{proj}}, c, q - q_0, \dot{q}, a_{t-1}]$ height grid (17×11)	48 187
h_t	$\{o_{t-k}\}_{k=1}^{15}$	15×48
p_t	$[\mu_{\text{fric}}, e, m_{\text{base}}, \Delta c, \mu_{\text{joint}}]$	18
z_m	morphology encoder output	$d = 11$

G. Training and Evaluation Protocol

Each parallel environment samples the descriptor m at the reset, applies it to the simulator, and rolls out the policy conditioned on $z = f_\psi(m)$. The same sampled m is passed through the morphology encoder and used consistently throughout the implementation. Training is performed on a single source robot template with morphology randomization applied to that template, while evaluation is conducted zero-shot on held-out robot morphologies m^* without retraining or hyperparameter tuning.

V. EXPERIMENTAL SETUP

A. Tasks and Observation Space

For our MorFiC approach, we have considered command velocity tracking for locomotion. We have considered linear and angular velocity and sampled it from the range, and we ran a curriculum over the command range to increase difficulty. And the episode ends after the fall, collapses, or timeouts. For detailed observations (see Table II), Each training environment is applied with the 11D morph vector in the simulation to represent a diverse set of robot behaviors. MorFiC maps m to latent through the encoder $z = E(m)$ and uses it to condition the critic via FiLM modulation.

B. Reward structure

Our reward structure is divided into three main categories: Task/Tracking, Penalties and stability shaping rewards, and the total reward sum is given by (6).

$$r_t = \sum_{i \in T} w_i r_t^{(i)} - \sum_{j \in P} w_j p_t^{(j)} + \sum_{k \in S} w_k s_t^{(k)}. \quad (6)$$

Task/Tracking rewards encourage the robot to complete the commanded locomotion objective. Specifically, we tracked the commanded linear velocity and the angular velocity using exponential rewards. (Details in the Appendix)

Penalties are assigned as a way to discourage unsafe movement, which could lead to collisions, bad gait, or physically collapse (like jerks, jerky motions, base collision, joint limit violation, etc). For example, we penalize body collisions

$$p_{\text{col}} = \sum_{b \in B} 1.(\|f_b\| > f_{\text{min}}), \quad (7)$$

TABLE III

SOTA COMPARISON. MORFiC IS THE SINGLE TRAIN ROBOT WHICH HAS HIGHEST ZERO-SHOT GENERALIZATION COUNT WHILE HITTING ALL THE KEY ATTRIBUTES. ZS (N): ZERO-SHOT MORPH TRANSFER (NUMBER OF TEST MORPHS). X-EMB: CROSS-EMBODIMENT TRANSFER. DOF: VARYING ACTION/OBS DIMENSIONS. MORPH @TEST / HIST @TEST: REQUIRES MORPHOLOGY PARAMETERS OR HISTORY BUFFER AT TEST TIME. VALUE-COND: CONDITIONING APPLIED IN VALUE PATHWAY. ROBUST: SAFETY/ROBUSTNESS-FOCUSED EVALUATION. HW (N): REAL-ROBOT TESTS (COUNT).

Paper	Train Robots (N)	Zero-shot (N)	Cross-Embod	Morph + DR Randomization	Morph @test	Hist @test	Critic conditioning	Robust/Safety	HW (N)
URMA [25]	16	✓(2)	✓	Morph + DR	✓	×	DescVec	✓	✓(1)
URMAv2 [26]	50	✓(5)	✓	Morph + DR	✓	×	DescVec	✓	✓(3)
LocoFormer [27]	Large-scale	✓(10)	✓	Morph	×	✓	Transformer	✓	✓(4)
ManyQuadrupeds [11]	16	✓(3)	✓	×	✓	×	×	✓	✓(2)
GenLoco [9]	Large-scale	✓(10)	✓	Morph + DR	✓	✓	None	✓	✓(3)
BodyTransformer [10]	1	×	×	×	✓	×	Transformer	×	✓(1)
RL2AC [28]	1	×	×	DR	×	✓	Latent z	✓	✓(1)
Emb. Scaling [29]	817	✓(204)	✓	Morph	×	✓	×	✓	✓(2)
MorFiC (Ours)	1	✓(7)	✓	Morph + DR	✓	✓	FiLM	✓	✓(2)

joint limit violations and is given by;

$$p_{\text{lim}} = \sum_i \left(\max(0, q_i - q_i^{\max}) + \max(0, q_i^{\min} - q_i) \right). \quad (8)$$

These help the robot in not deviating from the desired locomotion gait.

Stability Shaping. Motivated by our repeated failure on unseen morphologies, we introduce 3 lightweight stability rewards namely upright stability, CoP stability, and feet-contact stability to reduce catastrophic tipping and improve recovery.

- 1) **Upright stability.** Encourages recovery from large pitch/tilt by penalizing deviation from projected gravity.

$$s_{\text{upright}} = \exp\left(-\frac{\|\mathbf{g}_{xy}\|^2}{\sin^2(\theta_0)}\right). \quad (9)$$

- 2) **Center-of-pressure (CoP) stability.** Promotes balanced load distribution across the support polygon.

$$s_{\text{CoP}} = \exp\left(-\frac{\|\text{CoP} - \text{center}\|}{\tau}\right) \cdot 1(n_{\text{contact}} \geq 2). \quad (10)$$

- 3) **Feet-contact / stance-width stability.** Penalize overly narrow instances during unstable locomotion (caused by large tilt or rapid movement when unstable). We gate this using eqns. 11, 12.

$$\text{gate} = 1\left(\|\mathbf{g}_{xy}\|^2 > \eta \vee \|\mathbf{v}_{xy}\| > v_{\text{th}}\right), \quad (11)$$

and define

$$s_{\text{width}} = \text{gate} \cdot \exp\left(-\frac{\max(0, w_{\min} - w)}{\sigma_w}\right) + (1 - \text{gate}). \quad (12)$$

In addition to these components, we include a small set of rewards adapted from earlier work [30]. **All baselines were trained with the same reward**, so as to clearly isolate the performance difference caused by the poor approximation of the value function.

C. Baseline Comparison

We have compared 4 variants of PPO under identical training conditions like reward structure, morphology, domain randomization, and neural networks parameters:

- 1) **PPO:** No morphology conditioning
- 2) **Actor only:** Actor receives z
- 3) **Actor + Critic** Both receive via concatenation to observations
- 4) **MorFiC (FiLM Critic:** Actor gets z, but critic receives z via FiLM modulation).

In addition to analysis of PPO variants, we have also included recent work on morphology generalization and cross embodied locomotion URMA and URMAv2, LocoFormer, ManyQuadrupeds, GenLoco, BodyTransformer, RL2AC, and Embodiment Scaling Laws [25, 26, 27, 11, 9, 10, 28, 29] (Table III & IV).

D. Metrics

We utilized the following key metrics to measure the performance, stability, and speed of MorFiC trained policy.

1) *Max forward speed \bar{v} (m/s):* We measured the maximum stable forward velocity without tipping or falling on a given command velocity v_{cmd} , which was 1, 2, 2.5 m/s.

2) *Stable speed window T_{win} :* It is defined as the duration for which the robot runs at \bar{v} without any tripping or falling.

3) *Fall free duration T_{max} :* It's longest fall free duration for the given command velocity.

Normalized morphology distance. To analyze how transfer performance degrades with morphology shift, we have defined the normalized distance $d \in [0, 1]$ between target robot and training robot based on the 11-D morphology descriptor selected from Table I. We compute

$$d = \|\tilde{\mathbf{m}}_{\text{target}} - \tilde{\mathbf{m}}_{\text{train}}\|_2. \quad (13)$$

We use this for transfer loss analysis and not for training (refer to Fig. 5).

TABLE IV

ZERO-SHOT CROSS-ROBOT TRANSFER. TRAINING ON Go2; MORFiC ACHIEVES BEST STABLE SPEED ON ALL 6 ROBOTS, IMPROVING \bar{v} 0.26 m/s OVER STRONGEST BASELINES WHILE MAINTAINING A HIGH T_{\max} ; EVALUATION IS ZERO-SHOT ON ALL OTHER ROBOTS. WE REPORT STABLE AVERAGE SPEED \bar{v} (M/S) \uparrow , THE EVALUATION WINDOW USED T_{win} (S), AND THE LONGEST STABLE RUN T_{\max} (S) \uparrow . **BOLD** DENOTES THE BEST VALUE *per target robot*.

Target robot	PPO 1 (vanilla)			PPO 2 (Actor Only)			PPO 3 (Actor + Critic)			MorFiC		
	\bar{v} \uparrow (m/s)	T_{win} (s)	T_{\max} \uparrow (s)									
Go2 [†]	1.942	3.00	18.96	1.311	3.000	8.884	2.174	3.000	20.028	1.911	3.00	20.03
Go1	2.103	3.00	19.00	1.478	3.000	20.028	2.100	3.000	20.028	2.171	3.00	20.03
A1	1.969	3.00	19.04	0.365	0.920	0.920	1.698	3.000	5.462	2.286	3.00	20.03
AlienGo	0.470	3.00	18.92	0.650	1.240	1.240	0.439	3.000	20.028	0.993	3.00	9.08
B1	0.047	1.60	0.60	0.039	1.661	1.661	0.049	3.000	5.028	0.245	0.72	4.72
Cheetah	0.325	3.00	18.38	0.037	0.380	0.380	0.595	3.000	4.182	1.193	3.00	20.03
ANYmal	0.043	2.64	2.64	0.173	0.500	0.500	0.300	3.000	2.885	0.364	3.00	5.18

[†]Training morphology.

E. Training Details

We simulate Unitree Go2 for MorFiC evaluation, using the robot’s respective URDF file in the simulated environment (IsaacGym Simulator [31]). Each episode of simulation lasts for roughly 20 s with a total of 4000 parallel environments with a time-step of $dt = 0.005$. And, Commands $(v_x^{\text{cmd}}, v_y^{\text{cmd}}, \omega_z^{\text{cmd}})$ are provided at the beginning of each episode. We have adapted our code mainly from open-source repositories [30, 3]. A total of 400 million time steps were used in simulation training utilizing a Nvidia RTX 4090 laptop-based GPU. (Refer to the Appendix)

Curriculum. For curriculum, we utilize command curriculum expanding the popular fixed-rule-based [17] and game-inspired curriculum [3] to gradually increase difficulty. We use a history-aware update rule using Recurrent neural network. This curriculum is identical across all baselines.

Domain Randomization. To improve robustness and sim-to-real transfer in our setting we have used domain randomization [6] etc. and have randomized the following parameters joint friction, motor delays, sensor noise, etc.

VI. RESULTS

A. Zero-shot cross morphology transfer (Simulation)

We trained MorFiC on the single Unitree Go2 robot, with morphology randomization, and evaluated zero-shot on the other robots without any retraining or hyperparameter fine-tuning (Table IV). MorFiC is designed to improve transfer when there are poor critic value estimates. MorFiC delivers the most consistent gain over the PPO variants in terms of speed \bar{v} and stability T_{\max} . Overall, MorFiC improves performance on the OOD robots Cheetah (reaches 1.193 m/s) and Aliengo (approximately 0.993 m/s) and has comparatively better performance than the baselines, indicating that the actor alone or concatenating z with both actor and critic is insufficient. Overall Table IV and Figure 5 demonstrate that FiLM based conditioning is substantially more robust than latent concatenation for OOD morphology distribution.

B. Why MorFiC works: Critic and Advantage miscalibration

One of the key reasons why transfer fails is that critic fails in value estimation for the OOD robots, which leads to miscalibrated advantage function and subsequently worse PPO updates leading to unstable transfer. As per Fig. 3, the PPO variants are more in accordance with the advantage noise and have poor value estimates, where MorFiC has much better value estimates and which in turn improves the quality of the advantage as $\hat{A}_t = \hat{G}_t - V_\phi(x_t, m)$, leading to a more stable and generalizable policy. Figure 4 indicates that even if the instantaneous rewards are noisy, MorFiC has smoother value estimates, which highlights MorFiC’s utility in value function estimate as morphology shift.

C. Robustness

To fully measure robustness, we relate the transfer loss with d (Fig. 5) as the normalized distances d increase (i.e. the target robot deviates from the training robot), there is a decrease in all PPO variants, but the MorFiC performance was still better and is maintained higher T_{\max} than other PPO variants. MorFiC performs overall best on OOD morphology cheetah, where its inference is strongest (Table IV).

MorFiC vs previous Work. Table III identifies the two dominant ways to morphology generalization, which became popular recently. First, scaling i.e training on many robots or large models (eg. Transformers) [9] [27], [10]), which relies heavily on scale or compute. The second is a mixture of the intermediate number of robots and the test-time adaptation [25], [26], [28]. In contrast, MorFiC is single source (Train 1 robot) and deploys zero-shot on 7 target morphologies, including 2 real world deployment (Go1 & Go2), by directly addressing an underlying value function optimization issue under morphology shift.

D. Fairness (Parameters control)

In order to maintain the fairness of the evaluation, we kept all the necessary parameters like morphological and domain randomization parameters for the training robot, including all the PPO hyper-parameters, command curriculum ranges and

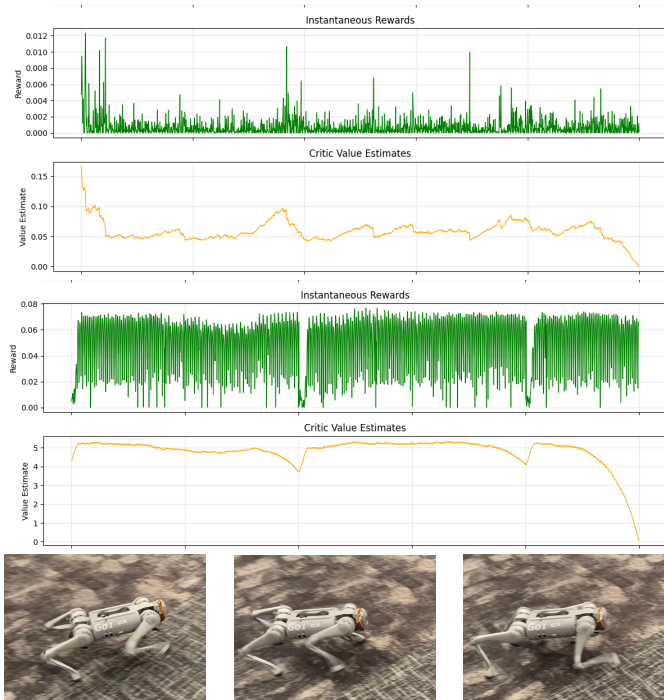


Fig. 4. Above figure shows representative reward and value trajectories during deployment on the Go1 robot. The MorFiC produces smooth value estimates (orange) (second row) that track the expected discounted returns from noisy instantaneous rewards (green). While non-MorFiC value estimates are noisy (first row), MorFiC’s morphology-conditioned critic maintains stable value predictions even on unseen morphologies.

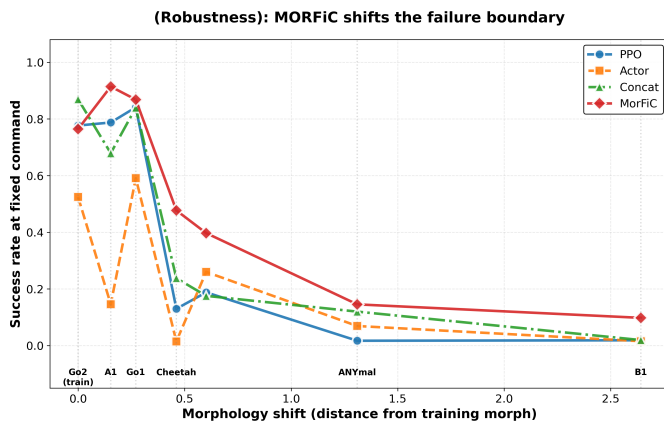


Fig. 5. From the above image, its clear that as the distance from the trained robot (Go2) increases there is decline in the performance but MorFiC still performs better than other variants of PPO significantly and also improved the generalization across OOD robots better than any other method.

reward functions, latent dimensions the same across all the variants. The key difference is in how the morph information is passed between the different variants (Section V-C)

VII. REAL-ROBOT RESULTS

A. Hardware setup & Zero-shot hardware results

Hardware Deployment. We deploy MorFiC policy on two hardware platforms namely Go1 and Go2 using an onboard LCM stack for state estimation and actions. We deploy the final policy on robots without any finetuning, MorFiC reaches

a nearly $\approx 1.4\text{--}1.7\text{ m/s}$ on Go1 robot over 10 trials with a success rate of over 80% while on Go2 robots it reaches roughly $\approx 1.1\text{--}1.3\text{ m/s}$. We deployed the same go2 policy weights which we used for zero-shot evaluation in sim-transfer.

Training robot robustness. To test the sensitivity of training morphology, we also train MorFiC on A1 robot and deploy zero-shot on both Go1 and Go2 robots. And the deployed policy reaches similar velocity ranges for both Go1 and Go2 robots with a success rate of 70%.

B. Failure Modes & Analysis

We have observed two categories of failures, System-level (generic) failure and Robot specific failures (Go2). The generic failures are mainly due to i) Latency and state-estimator drift, ii) Contact mismatch during runs (either foot slips or uneven gait). For robot specific failures, Go2 exhibits a reduced speed and also a higher failure rate under our current deployment pipeline. We have attributed those failures primarily due to observation mismatch or action scaling issues or aggressive safety layers on Go2

MorFiC reduces policy specific failure even in unseen zero-shot, for example, Go2 trained policy transfer to Go1 or A1 trained policy on both Go1 or Go2, remains functional, but system level constraints still reduce speed and trigger failures.

VIII. ABLATIONS & LIMITATIONS

A. Ablations

Table IV isolates the key benefit of MorFiC vs. PPO variants:

- 1) **Actor Only:** Based on speed and T_{win} results indicate that its brittle and insufficient compared to PPO.
- 2) **Concatenation** helps in some case, for example. Actor + critic improves speed compared to PPO (0.595 vs 0.325 m/s), but still collapse after $T_{max} = 4.18\text{ s}$.
- 3) **FiLM critic** is the robust choice for both in-family and OOD robots as it improves speed and stability (Cheetah $\bar{v} = 1.193\text{ m/s}$ & $T_{max} = 20.03\text{ s}$).

B. Limitations & Future work

One of the key limitations of our work is that MorFiC transfer success drops significantly on the extreme out of distribution morphology, for example Anymal robot, especially B1, as the incidents of tipping and falling increases and along with degraded speed or fail to sustain a stable posture. In addition to that, we currently study MorFiC transfer on the quadrupeds and locomotion tasks only, we have not evaluated bipeds/humanoids. As an expansion of our work, we would like to extend MorFiC to bipedal and humanoid locomotion, in order to move towards an even better and more robust single source trained policy for various morphologies including bipedal and humanoids.

IX. CONCLUSION

We have studied the zero-shot cross morphology problem and found that transfer failure is strongly driven by the critic function miscalibration, leads to biased advantage, and ultimately leads to poor PPO updates. MorFiC addresses this by conditioning the critic function via FiLM and modulating by a learned morphology latent. By improving value function estimates, we can get better generalization results instead of focusing on a very high number of morphology mixes or using heavier networks like transformers. Based on our results (Table IV, supported by Figures 3-5), MorFiC improves stability, speed, and OOD generalization better than any PPO variant while remaining highly competitive in family robot transfer and transfers zero-shot to 2 real robots (Go1 & Go2).

REFERENCES

- [1] J. Hwangbo, J. Lee, A. Dosovitskiy, D. Bellicoso, V. Tsounis, V. Koltun, and M. Hutter, "Learning agile and dynamic motor skills for legged robots," *Science Robotics*, vol. 4, no. 26, 2019.
- [2] J. Lee, J. Hwangbo, L. Wellhausen, V. Koltun, and M. Hutter, "Learning quadrupedal locomotion over challenging terrain," *Science Robotics*, vol. 5, no. 47, 2020.
- [3] N. Rudin, D. Hoeller, P. Reist, and M. Hutter, "Learning to walk in minutes using massively parallel deep reinforcement learning," in *Conference on Robot Learning (CoRL)*, 2022.
- [4] G. Pan, Q. Ben, Z. Yuan, G. Jiang, Y. Ji, S. Li, J. Pang, H. Liu, and H. Xu, "Roboduet: Learning a cooperative policy for whole-body legged loco-manipulation," *IEEE Robotics and Automation Letters*, 2025.
- [5] S. Yang, Z. Fu, Z. Cao, G. Junde, P. Wensing, W. Zhang, and H. Chen, "Multi-loco: Unifying multi-embodiment legged locomotion via reinforcement learning augmented diffusion," in *Proceedings of the Conference on Robot Learning (CoRL)*, 2025.
- [6] J. Tan, T. Zhang, E. Coumans, S. Ha, J. Geijtenbeek, and C. K. Liu, "Sim-to-real: Learning agile locomotion for quadruped robots," in *Robotics: Science and Systems (RSS)*, 2018.
- [7] X. B. Peng, M. Andrychowicz, W. Zaremba, and P. Abbeel, "Sim-to-real transfer of robotic control with dynamics randomization," in *IEEE International Conference on Robotics and Automation (ICRA)*, 2018.
- [8] J. Tobin, R. Fong, A. Ray, J. Schneider, W. Zaremba, and P. Abbeel, "Domain randomization for transferring deep neural networks from simulation to the real world," in *IEEE/RSJ International Conference on Intelligent Robots and Systems (IROS)*, 2017.
- [9] G. Feng, H. Zhang, Z. Li, X. B. Peng, A. Kanazawa, and S. Levine, "Genloco: Generalized locomotion controllers for quadrupedal robots," in *Conference on Robot Learning (CoRL)*, 2023.
- [10] C. Sferrazza and L. Righetti, "Learning generalizable locomotion for quadrupedal robots with body transformer," in *Robotics: Science and Systems (RSS)*, 2023.
- [11] S. Shafiee, G. Bellegarda, and A. Ijspeert, "Manyquadrupeds: Learning a single locomotion policy for diverse quadruped robots," in *IEEE International Conference on Robotics and Automation (ICRA)*, 2024.
- [12] J. Hejna, A. Xie, P. Abbeel, A. D. Dragan, J. Gao, and D. Sadigh, "Hierarchically decoupled imitation for morphological transfer," in *Proceedings of the 37th International Conference on Machine Learning (ICML)*. PMLR, 2020.
- [13] B. Trabucco, M. Phielipp, and G. Berseth, "Anymorph: Learning transferable policies by inferring agent morphology," in *Proceedings of the 39th International Conference on Machine Learning (ICML)*. PMLR, 2022.
- [14] J. Schulman, F. Wolski, P. Dhariwal, A. Radford, and O. Klimov, "Proximal policy optimization algorithms," in *International Conference on Learning Representations (ICLR)*, 2017.
- [15] P. Henderson, R. Islam, P. Bachman, J. Pineau, D. Precup, and D. Meger, "Deep reinforcement learning that matters," in *AAAI Conference on Artificial Intelligence*, 2018.
- [16] E. Perez, F. Strub, H. De Vries, V. Dumoulin, and A. Courville, "Film: Visual reasoning with a general conditioning layer," in *Proceedings of the AAAI conference on artificial intelligence*, vol. 32, no. 1, 2018.
- [17] G. B. Margolis, G.-Z. Yang, K. Paigwar, T. Chen, and P. Agrawal, "Rapid locomotion via reinforcement learning," *The International Journal of Robotics Research*, vol. 43, no. 4, pp. 572–587, 2024.
- [18] A. Kumar, A. Agarwal, A. Singh, F. Ebert, Y. Duan, C. Finn, and S. Levine, "Learning to walk with rapid motor adaptation," in *Robotics: Science and Systems (RSS)*, 2021.
- [19] H. Zhao, Y. Wang, and T. Chen, "Zero-shot learning for robust quadrupedal locomotion via recurrent reinforcement learning," in *IEEE International Conference on Robotics and Automation (ICRA)*, 2024.
- [20] S. Liu, D. Xu, and L. Pinto, "Understanding and mitigating interference in multi-task reinforcement learning," in *Conference on Robot Learning (CoRL)*, 2023.
- [21] F. Doshi-Velez and G. Konidaris, "Hidden parameter markov decision processes: A semiparametric regression approach for discovering latent task parametrizations," in *Proceedings of the 30th AAAI Conference on Artificial Intelligence (AAAI)*, 2016.
- [22] A. Gupta, S. Savarese, S. Ganguli, and L. Fei-Fei, "Metamorph: Learning universal controllers with transformers," in *International Conference on Learning Representations (ICLR)*, 2022.
- [23] T. Yu *et al.*, "Gradient surgery for multi-task learning," in *NeurIPS*, 2020.
- [24] J. Schulman *et al.*, "High-dimensional continuous control using generalized advantage estimation," in *ICLR*, 2016.
- [25] N. Bohlinger, G. Czechmanowski, J. Peters, and D. Tateo, "One policy to run them all: An end-to-end learning approach to multi-embodiment locomotion," in *Conference*

on Robot Learning (CoRL), 2024.

- [26] N. Bohlinger and J. Peters, “Multi-embodiment locomotion at scale with extreme embodiment randomization,” *arXiv preprint arXiv:2509.02815*, 2025.
- [27] M. Liu, D. Pathak, and A. Agarwal, “Locoformer: Generalist locomotion via long-context adaptation,” *arXiv preprint arXiv:2509.23745*, 2025.
- [28] S. Lyu, X. Lang, H. Zhao, H. Zhang, P. Ding, and D. Wang, “Rl2ac: Reinforcement learning-based rapid online adaptive control for legged robot robust locomotion,” in *Proceedings of the Robotics: Science and Systems*, 2024.
- [29] R. Doshi, H. Walke, O. Mees, S. Dasari, and S. Levine, “Scaling cross-embodied learning: One policy for manipulation, navigation, locomotion and aviation,” *arXiv preprint arXiv:2408.11812*, 2024.
- [30] G. B. Margolis and P. Agrawal, “Walk these ways: Tuning robot control for generalization with multiplicity of behavior,” in *Conference on Robot Learning*. PMLR, 2023, pp. 22–31.
- [31] V. Makoviychuk, L. Wawrzyniak, Y. Guo, M. Lu, K. Nguyen, M. Macklin, G. Lukamowicz, Y. State, J. Liang, J. Zhu *et al.*, “Isaac gym: High performance GPU-based physics simulation for robot learning,” *arXiv preprint arXiv:2108.10470*, 2021.

Term	Definition	Weight
r_{lin}	$4 \exp\left(-\frac{\ \mathbf{v}_{xy}^{cmd} - \mathbf{v}_{xy}\ ^2}{\sigma_{\text{lin}}}\right)$	w_{lin}
r_{yaw}	$\exp\left(-\frac{(\omega_z^{cmd} - \omega_z)^2}{\sigma_{\text{yaw}}}\right)$	w_{yaw}
p_{v_z}	$(v_z)^2$	w_{v_z}
$p_{\omega_{xy}}$	$\ \omega_{xy}\ ^2$	w_{ω}
p_{ori}	$\ \mathbf{g}_{xy}\ ^2$	w_{ori}
p_{τ}	$\ \boldsymbol{\tau}\ ^2$	w_{τ}
$p_{\dot{q}}$	$\left\ \frac{\dot{q}_{t-1} - \dot{q}_t}{\Delta t}\right\ ^2$	$w_{\dot{q}}$
$p_{\Delta a}$	$\ a_{t-1} - a_t\ ^2$	$w_{\Delta a}$
p_{coll}	$\sum_{b \in \mathcal{B}} \mathbb{I}(\ \mathbf{f}_b\ > 0.1)$	w_{coll}
p_{jl}	$\sum_i [(q_i - q_i^{\min})_- + (q_i - q_i^{\max})_+]$	w_{jl}
r_{upright}	$\exp\left(-\frac{\ \mathbf{g}_{xy}\ ^2}{\sin^2(\theta_0)}\right), \theta_0=0.3$	w_{upright}
r_{cop}	$\mathbb{I}(n_c \geq 2) \exp\left(-\frac{\ \text{CoP-center}\ }{\tau}\right), \tau=0.10$	w_{cop}
r_{width}	$(\text{yaw-frame}) \exp\left(-\frac{(w_{\min} - w)_+}{\sigma_w}\right)$ (gated)	w_{width}
r_{gaitF}	$-\frac{1}{4} \sum_i (1 - d_i) (1 - \exp(-f_i^2/\sigma_F))$	w_{gaitF}
r_{gaitV}	$-\frac{1}{4} \sum_i d_i (1 - \exp(-\ \dot{\mathbf{x}}_i\ ^2/\sigma_V))$	w_{gaitV}
p_{slip}	$\sum_i \mathbb{I}(c_i) \ \dot{\mathbf{x}}_{i,xy}\ ^2$	w_{slip}
p_{impact}	$\sum_i \mathbb{I}(c_i) \text{clip}(\dot{z}_{i,t-1}, -100, 0)^2$	w_{impact}
p_f	$\sum_i (\ \mathbf{f}_i\ - f_{\max})_+$	w_f
p_q	$\ q - q^0\ ^2$	w_q
$p_{\dot{q}}$	$\ \dot{q}\ ^2$	$w_{\dot{q}}$
r_{jump}	$-(z - (h^{cmd} + h_0))^2$	w_{jump}
r_{raibert}	$\ \mathbf{x}_{\text{foot}}^{des} - \mathbf{x}_{\text{foot}}\ ^2$ (body yaw frame)	w_{raibert}

TABLE V

REWARD TERMS USED IN OUR MORFIC LOCOMOTION OBJECTIVE. w_k ARE SET IN THE REWARD CONFIGURATION; FIXED SCALINGS APPEARING IN CODE (E.G., THE FACTOR 4 IN r_{LIN}) ARE SHOWN EXPLICITLY.

APPENDIX A

REWARD TERMS AND WEIGHTS

We shape our MorFiC rewards as a weighted sum of (i) command tracking terms for linear and angular velocities using exponential, (ii) stability rewards that encourage upright posture and dynamic balance via a center-of-pressure (CoP) proximity reward, (iii) gait/contact shaping terms that match desired contact schedules by penalizing unwanted swing forces and stance-phase foot velocities and a detailed definition and weights are given in Table V.

APPENDIX B

PPO + MORFIC HYPERPARAMETERS

A. Policy and critic architectures

We use an actor–critic policy with separate MLP trunks for the actor and critic. Unless stated otherwise, all hidden layers use **ELU** activations. The actor and critic base networks each use hidden dimensions [512, 256, 128] and the policy outputs actions.

For morphology conditioning, we encode the morphology vector $m \in \mathbb{R}^{d_m}$ using a lightweight **MorphologyEncoder** $z = \phi(m)$ implemented as a 2-layer MLP with ELU activations. The critic is conditioned via **FiLM** modulation at each critic hidden layer. To ensure stable early training, the FiLM head is initialized to output near-zero modulation (final layer

PPO setting	Value
Discount γ	0.99
GAE λ	0.95
Clip ϵ	0.2
Entropy coeff.	0.01
Value loss coeff.	1.0
Clipped value loss	True
Learning rate	1×10^{-3}
Schedule	adaptive (KL-targeted)
Target KL	0.01
Epochs / update	5
Mini-batches / update	4
Grad norm clip	1.0

TABLE VI

PPO HYPERPARAMETERS USED IN ALL BASELINE AND MORFIC EXPERIMENTS.

Module	Spec
Actor MLP	[512, 256, 128], ELU
Critic MLP trunk	[512, 256, 128], ELU
Init action std. σ_0	1.0
MorphologyEncoder	$d_m \rightarrow 128 \rightarrow 64$ (ELU)
FiLM per layer	$64 \rightarrow 128 \rightarrow 2H$ (ELU)
FiLM type	residual: $h \leftarrow h(1 + \gamma) + \beta$
FiLM init	last layer weights, bias = 0
FiLM scale	0.1
Decoder	disabled

TABLE VII

POLICY/CRITIC ARCHITECTURE AND MORPHOLOGY-CODITIONING DETAILS. H IS THE HIDDEN WIDTH OF THE MODULATED CRITIC LAYER.

weights and biases set to zero), making the critic start close to the unconditioned baseline. We use a FiLM output scale of 0.1.

B.2 PPO hyperparameters

We train with PPO using clipped objectives and a clipped value loss. We use discount $\gamma = 0.99$, GAE parameter $\lambda = 0.95$, clipping parameter $\epsilon = 0.2$, entropy coefficient 0.01, value loss coefficient 1.0, and gradient norm clipping at 1.0. Optimization uses an adaptive learning rate schedule that targets KL divergence $\text{KL}_{\text{target}} = 0.01$, with a base learning rate 10^{-3} . Each update uses 5 learning epochs and 4 mini-batches.

APPENDIX C. DOMAIN RANDOMIZATION

We apply domain randomization during training to improve robustness and sim-to-real transfer. Randomization is applied periodically with the interval 10 s (rigid-body properties are randomized after initialization). We randomize the properties of contact with the ground by sampling the friction coefficient uniformly from [0.5, 1.25]. We inject external disturbances by pushing the robot at fixed intervals of 15 s with a maximum planar push velocity of 1.0 m/s. To model actuation/communication delay, we randomize action latency using a history buffer of up to 6 timesteps (randomized lag timesteps enabled).